

THE ANGULAR CLUSTERING OF LYMAN-BREAK GALAXIES AT REDSHIFT $z \sim 3$ ¹

MAURO GIAVALISCO²

Observatories of the Carnegie Institution of Washington, 813 Santa Barbara Street, Pasadena,
CA 91101

e-mail: mauro@ociw.edu

CHARLES C. STEIDEL^{3,4} AND KURT L. ADELBERGER

Palomar Observatory, California Institute of Technology, Mail Stop 105-24, Pasadena, CA 91125

e-mail: ccs,kla@astro.caltech.edu

MARK E. DICKINSON⁵

Department of Physics and Astronomy, The Johns Hopkins University, N. Charles St., Baltimore,
MD 21218

e-mail: med@stsci.edu

MAX PETTINI

Royal Greenwich Observatory, Madingley Road, Cambridge, CB3 0EZ, UK

e-mail: pettini@ast.cam.ac.uk

MELINDA KELLOGG

Palomar Observatory, California Institute of Technology, Mail Stop 105-24, Pasadena, CA 91125

e-mail: mk@astro.caltech.edu

ABSTRACT

We have measured the angular correlation function $w(\theta)$ for a sample of 871 Lyman-break galaxies (LBGs) in five fields at redshift $z \sim 3$. Fitting the power-law $A_w \theta^{-\beta}$ to a weighted average of $w(\theta)$ from the five fields over the range $12 \lesssim \theta \lesssim 330$ arcsec, we find $A_w \sim 2 \text{ arcsec}^\beta$ and $\beta \sim 0.9$. The slope is, within the errors, the same as for galaxy samples in the local and intermediate redshift universe, and a

¹Based on observations obtained at the Palomar Observatory, at the Kitt Peak National Observatory and at the W. M. Keck Observatory, which is operated jointly by the California Institute of Technology and the University of California.

²Hubble Fellow.

³Alfred P. Sloan Foundation Fellow.

⁴NSF Young Investigator.

⁵Allan C. Davis Fellow, also with the Space Telescope Science Institute.

slope $\beta = 0.25$ or shallower is ruled out by the data at the 99.9% confidence level. Because $N(z)$ of LBGs is well determined from 376 spectroscopic LBG redshifts, the real-space correlation function can be accurately derived from the angular one through the Limber transform. The inversion of $w(\theta)$ is rather insensitive to the still relatively large uncertainties on A_ω and β , and the spatial correlation length is much more tightly constrained than either of these parameters. We estimate $r_0 = 3.3_{-0.6}^{+0.7}$ ($2.1_{-0.5}^{+0.4}$) $h^{-1}\text{Mpc}$ (comoving) for $q_0 = 0.1$ (0.5) at the median redshift of the survey, $\bar{z} = 3.04$ (h is in units of $100 \text{ km s}^{-1} \text{ Mpc}^{-1}$ throughout this paper). The observed comoving correlation length of LBGs at $z \sim 3$ is comparable to that of present-day spiral galaxies and is only $\sim 50\%$ smaller than that of present-day ellipticals; it is as large or larger than any measured in recent intermediate-redshift galaxy samples ($0.3 \lesssim z \lesssim 1$). By comparing the observed galaxy correlation length to that of the mass predicted from CDM theory, we estimate a linear bias for LBGs of $b \sim 1.5$ (4.5) for $q_0 = 0.1$ (0.5), in broad agreement with our previous estimates based on preliminary spectroscopy. The strong clustering and the large bias of the LBGs are consistent with biased galaxy formation theories and provide additional evidence that these systems are associated with massive dark matter halos. The results of the clustering of LBGs at $z \sim 3$ emphasize that apparent evolution in the clustering properties of galaxies may be due as much to variations in effective light-to-mass bias parameter among different galaxy samples as to evolution in the mass distribution through gravitational instability.

Subject headings: cosmology: observations — galaxies: formation — galaxies: evolution — galaxies: distances and redshifts

1. INTRODUCTION

In most cosmological models, galaxies are expected to be biased tracers of the underlying mass-density field, with the level of light-to-mass bias being a function of the galaxy mass; more massive galaxies would tend to populate volumes of space with a higher overall mass density, and, as a consequence, would be characterized by a stronger spatial clustering than less massive systems (e.g. Kaiser 1984; Mo & White 1996). Furthermore, the bias of galaxies respect to the mass is expected to evolve with cosmic time as a result of gravitational growth of density perturbation and hierarchical merging (Matarrese *et al.* 1997; Mann, Peacock & Heavens 1997; Bagla 1997). Empirically, it has been known for some time that different types of galaxies do indeed cluster differently; numerous large galaxy redshift surveys (Davis *et al.* 1988; Hamilton 1988; Santiago & Da Costa 1990; Loveday *et al.* 1995; Tucker *et al.* 1996; Valotto & Lambdas 1997) in the local universe have shown that early-type galaxies (E/S0) are more strongly clustered than later types (Sp/Irr), with a two-point correlation function that is generally steeper and a correlation length ~ 2 times larger. A similar trend with the absolute luminosities of the galaxies has also been

observed (Park *et al.* 1994).

In the past few years, several deep redshift surveys have probed field galaxies in the intermediate-redshift universe (e.g. Lilly *et al.* 1995; Cowie, Hu & Songaila 1995). These find similar clustering segregation as in the local universe, with the redder and more luminous systems more strongly clustered than their bluer and fainter counterparts (Le Fèvre *et al.* 1996; Carlberg *et al.* 1997), and detect apparent evolution in galaxy clustering, with a comoving correlation length r_0 that is three times smaller at $z \sim 1$ than in local samples. If the galaxies in these samples at different redshifts all had the same bias with respect to the mass distribution, then the observed differences in galaxy clustering trace the evolution of mass clustering, and could be used to constrain cosmology; however, it is difficult to understand the mix of galaxy masses included in magnitude limited surveys as a function of redshift. One might hope that a sample’s bias would not depend strongly on how it was selected, but if this were the case then different redshift surveys would currently be in quantitative disagreement with each other (Carlberg *et al.* 1997). It seems likely, then, that a sample-dependent (both because of redshift effects and selection criteria) light-to-mass bias could be at least partly responsible for the observed “evolution” of galaxy clustering with redshift, and in this case it would be difficult to draw cosmological conclusions from those surveys.

Recently, it has become possible to identify large numbers of galaxies in a narrow redshift range using photometric techniques (e.g. Connolly *et al.* 1995, Steidel *et al.* 1996a, Madau *et al.* 1996). In contrast to traditional magnitude-limited surveys, which contain a wide range of galaxies over a large interval of time, and likely different mixtures of galaxies at different redshifts, a sample selected in this way provides a snapshot of the locations of similar galaxies over a small span of time. As a result, the observed clustering is much easier to interpret. An example of a photometric redshift technique is the Lyman-break technique (Steidel & Hamilton 1993, Steidel, Pettini, & Hamilton 1995, Steidel *et al.* 1996a, Giavalisco *et al.* 1996, Madau *et al.* 1996) which selects the brightest star-forming (and relatively dust-free) galaxies at high redshift. It is still unclear what the lower redshift counterparts of these Lyman-break galaxies would be, and so one cannot easily draw cosmological conclusions by comparing the clustering strength of Lyman-break galaxies to the clustering strength of a lower-redshift sample; but we can use the sample for the more modest goal of constraining theories of galaxy formation. In particular there is a great deal of fruitful work to be done comparing the properties of this well-defined high-redshift sample with the predictions of numerical and semi-analytic models (Baugh *et al.* 1998, Jing & Suto 1998, Governato *et al.* 1998).

In a previous paper (Steidel *et al.* 1998, Paper 1) we described a large concentration of LBGs in redshift space discovered in one of our survey fields, and argued that such a concentration would not exist in standard CDM cosmogonies unless LBGs were very biased tracers of mass. In the present paper, we present a complementary angular clustering analysis of the LBG candidates in 5 of our survey fields, which can be used in conjunction with the spectroscopic redshift distribution to estimate the spatial correlation function of the Lyman-break population at $z \sim 3$. Again, we

will find that these galaxies are much more strongly clustered than the mass would be according to models of hierarchical structure formation. Such a strong clustering of forming galaxies is actually in agreement with predictions of models in which LBGs are associated with relatively rare and massive dark matter halos (e.g., Baugh *et al.* 1997, Mo & Fukugita 1996, Jing & Suto 1998).

2. LYMAN-BREAK GALAXIES

The Lyman-break technique uses color selection to identify high-redshift galaxies through multi-band imaging across the 912 Å Lyman-continuum discontinuity. Details of the technique have been presented elsewhere (e.g. Steidel & Hamilton 1993; Steidel, Pettini & Hamilton 1995; Madau *et al.* 1996) and here we only briefly review them. At $z \gtrsim 2.5$ the Lyman limit is redshifted far enough into the optical window to be observable in broad-band ground-based photometry. By placing filters on either side of the redshifted Lyman limit one can find high-redshift objects by their strong spectral breaks. In our implementation of the technique we use a custom photometric system, $U_n G \mathcal{R}$ (Steidel & Hamilton 1993) optimized for selecting LBGs with $z \sim 3$. An initial selection region of the $[G - \mathcal{R}, U_n - G]$ plane was chosen based on the expected colors of moderately unreddened star-forming galaxies computed using stellar population synthesis codes (Bruzual & Charlot 1996), and including the effects of the opacity of interstellar gas and intervening absorption by H I (Steidel *et al.* 1995; see also Madau 1995). Our selection criteria were subsequently verified and refined after extensive spectroscopy with the Low Resolution Imaging Spectrograph (Oke *et al.* 1995) on the W.M. Keck telescope.

In this paper an object is considered a Lyman-break galaxy if its colors satisfy

$$(U_n - G) \geq 1.0 + (G - \mathcal{R}); \quad (U_n - G) \geq 1.6; \quad (G - \mathcal{R}) \leq 1.2, \quad (1)$$

with an additional requirement $\mathcal{R} < 25.5$ imposed to produce a reasonably complete sample that is suitable for spectroscopic follow-up. Magnitudes are in the AB scale (Oke & Gunn, 1983). We have found that at least 75% of the objects meeting these criteria are indeed high-redshift galaxies. Figure 1 shows the redshift distribution $N(z)$ for all 376 spectroscopically identified galaxies selected with these criteria. The median redshift is $\bar{z} = 3.04$ and the standard deviation is $\sigma_z = 0.27$; approximately 90% of the galaxies have $2.6 \lesssim z \lesssim 3.4$, and none have $z < 2.2$. About 5% of the objects meeting these criteria are stars; almost all of these are brighter than $\mathcal{R} \sim 24$. The remaining 20% of objects meeting these criteria have not been identified because of low S/N. Our success in obtaining a redshift has no obvious dependence on luminosity or color.

For the purpose of measuring angular clustering we have restricted our sample to candidates from the larger and deeper fields of our survey, whose salient features are summarized in Table 1. While each of the fields will be treated independently in the analysis below, the surface density of faint galaxies, and the median colors for all detected objects in each field, are consistent with one another after correction for Galactic reddening. Each of our images typically has seeing in the range $0''.8 - 1''.3$, and reaches 1σ surface brightness fluctuations in 1 arcsec^2 apertures of ~ 29.1 ,

29.2, and 28.6 magnitudes/arcsec² in the U_n , G , and \mathcal{R} bands, respectively. However, for objects fainter than $\mathcal{R} \approx 25$ small differences in the depth of the U_n images can influence the surface density of the faintest LBG candidates because of the large dynamic range required to flag objects with significant continuum breaks. For this reason, we caution that the surface density of LBG candidates can have a small dependence on the quality of the images in a particular field.

We are in the process of obtaining spectra of LBG candidates in each of these fields using the Keck telescopes; in the present work, we make use only of the redshift distribution for our spectroscopic survey as a whole. We defer to a future paper an analysis of the clustering in each field using the full redshift information (Adelberger *et al.* 1998, in preparation).

Most of the fields chosen for our LBG survey are high latitude, low Galactic reddening fields that have been the subject of other faint galaxy studies; particularly relevant to our choice of fields was the existence of deep WFPC-2 images in the *HST* archive.

The largest field is 1415+527, which is centered on a deep *HST*+WFPC-2 pointing and also contains several of the pointings of the “Groth strip”. The field has also been studied by Connolly *et al.* (1997) for their photometric-redshift technique, and by the Canada-France redshift survey (Lilly *et al.* 1995). Our images were obtained using the prime focus camera on the Mayall 4-m telescope at Kitt Peak during 1996 May and cover an area of 15×15 arcmin²; the \mathcal{R} image was supplemented with a mosaic of images (in order to cover the whole KPNO 4m field of view) obtained at the Palomar 5m Hale telescope with the COSMIC prime focus camera in 1997 March.

The 2237+116 field (DSF2237) was chosen by us as region with low Galactic extinction and few bright stars which could be observed efficiently from both Palomar and Keck observatories in the late summer/early fall observing season. To our knowledge, no other faint galaxy studies have been conducted here. The imaging data were obtained in 1997 August with the Palomar 5m telescope; the total region studied consists of two abutting pointings, each $9'$ by $9'$, aligned in the E-W direction.

Like the 2237+116 field, the 2215+000 field consists of two COSMIC abutting pointings which have in this case been aligned along the North-South direction. The images were obtained in 1995 August, 1996 August, and 1997 August. The northern pointing is centered on the “SSA22” field of Cowie *et al.* (1995) and overlaps somewhat with the region studied as part of the CFRS redshift survey “22 hour” field (Lilly *et al.* 1995). It also includes several moderately deep *HST*+WFPC-2 pointings (Cowie *et al.* 1996; Schade *et al.* 1995). In Paper 1 we have presented a preliminary analysis of LBG spectroscopy in this region.

The 1234+625 (Hubble Deep Field, or HDF; Williams *et al.* 1996) and 0050+123 (“Caltech Deep Field”, or CDF) fields were obtained as single pointings with COSMIC. The observations were carried out during March and April 1996 in the former and during October 1996 in the latter, respectively. The HDF has been extensively followed-up with Keck spectroscopy by several groups (Cowie *et al.* 1997; Cohen *et al.* 1996), including observations of Lyman-break galaxies identified with *HST* (Steidel *et al.* 1996b; Lowenthal *et al.* 1997). In the CDF, Cohen *et al.* (1996)

have obtained redshifts, primarily in the $0.3 \leq z \leq 1$ range, as part of the “Caltech Deep Redshift Survey”; this field was chosen by both Cohen *et al.* and by us because of the existence of a deep WFPC-2 “Medium Deep Survey” image at the center. For both the HDF and the CDF our images cover a region much larger than, but including, the *HST* pointings.

3. THE MEASURE OF $w(\theta)$

The angular correlation function $w(\theta)$ is defined in terms of the excess probability over the random (Poisson) distribution of finding a companion in an angular shell of size $d\Omega$ placed at an angular separation θ from a selected galaxy, given the surface density of sources \mathcal{N} (Peebles 1980):

$$dP = \mathcal{N} [1 + w(\theta)] d\Omega. \quad (2)$$

Usually $w(\theta)$ is measured by comparing the observed number of galaxy pairs at a given separation θ to the number of pairs of galaxies independently and uniformly distributed over the same geometry as the observed field. A number of statistical estimators of $w(\theta)$ have been proposed (e.g. see Landy & Szalay 1993) in an attempt to minimize random and systematic errors.

We considered the two estimators

$$w(\theta) = \frac{DD(\theta)}{DR(\theta)} - 1 \quad (3)$$

and

$$w(\theta) = \frac{DD(\theta) - 2DR(\theta) + RR(\theta)}{RR(\theta)}, \quad (4)$$

proposed by Peebles (1980) and Landy & Szalay (1993), respectively (PB and LS in the following), where $DD(\theta)$ is the number of pairs of observed galaxies with angular separations in the range $(\theta, \theta + \delta\theta)$, $RR(\theta)$ is the analogous quantity for the homogeneous (random) catalog, and $DR(\theta)$ is the number of observed-random cross pairs. Both of these statistics produce estimates of $w(\theta)$ which are biased low by a factor (the “integral constraint”) $I \simeq 1 + O((\theta_0/\theta_{\max})^\beta)$, where $w(\theta_0) = 1$ (Peebles 1974), but (as we will see) $\theta_0 \ll \theta_{\max}$ and we will neglect this small correction. The properties of the two statistics are discussed by Landy & Szalay (1993). Relevant to our analysis is the fact that the variance of the LS estimator is smaller than the PB one, and is close to the variance of a Poisson distribution. In addition, the LS estimator should be less sensitive to edge effects and the presence of spurious variations of galaxy surface density (see below). We measured $w(\theta)$ using both estimators to test for the presence of such systematics.

We measured the correlation function using different techniques, as detailed below. The analysis was carried out using two independently written programs, finding virtually identical results. In each case we computed $w(\theta)$ from each individual field and then computed a weighted average using inverse variance weighting; it made little difference if we used Poisson or bootstrap variance (Ling, Barrow & Frenk 1986). The error bars on the average correlation function are

the rms field-to-field variation in the estimated individual $w(\theta)$ divided by $\sqrt{N_{\text{fields}}}$; Poisson and bootstrap errors have comparable size. Masking the regions around bright stars and galaxies where we could have not detected LBGs had a negligible effect on the results.

We subsequently fitted the weighted average to the power law $A_\omega \theta^{-\beta}$ with Levenberg-Marquardt nonlinear least-squares (Press *et al.* 1992). To estimate confidence intervals on the parameters A_ω and β , we generated a large ensemble of random realizations (100,000) of the measured $w(\theta)$, assuming normal errors, and calculated best fit parameter values for each of these synthetic data sets (e.g. Press *et al.* 1992 §15.6). We found that the fitted parameters depend somewhat on the choice of the binning used to compute $w(\theta)$, and to take this additional source of uncertainties into account we have included the effects of a randomly variable binning into the Monte Carlo simulations. Table 2 lists the results. Because the fitted parameters are strongly covariant, the 68% confidence intervals are misleadingly large, particularly the one relative to A_ω ; as we shall see, the comoving correlation length r_0 is much more tightly constrained than either A or β individually.

Figure 2 shows the weighted average estimates of $w(\theta)$ obtained from both the PB and LS estimators. For clarity, the error bars are plotted separately from the data points, in the upper part of the figure. A number of potential sources of systematic errors can affect the estimate of $w(\theta)$ and we now describe the techniques that we have adopted to test for their presence.

3.1. Spurious Sources

Systematic contamination from spurious sources, i.e. sources physically unrelated to the Lyman-break galaxies, is relatively easy to take into account. Only $\sim 75\%$ of the spectroscopically observed Lyman-break candidates have been shown to be at $z \sim 3$. About 5% are stars and the remaining 20% have not been identified. The unidentified 20% have spectra and colors consistent with their being at $z \sim 3$, but in the worst case a fraction $f \sim 0.25$ of the photometrically selected objects could lie at redshifts outside of our primary selection window. If these objects were not clustered our estimate of $w(\theta)$ would be low by a factor of $1/(1-f)^2 \simeq 1.56$. We will refer to this as the case of “maximum contamination”.

3.2. Field-to-Field Variations

Particularly insidious are slight variations in detection probability across the chip due to structure in flatfields, optical aberrations, software performance, and so on. If uncorrected, the resulting density gradients can mimic galaxy clustering. We have tested for the presence of such effects by using the locations of non-LBG galaxies instead of a uniform (random) distribution when estimating DR and RR . Because these faint galaxies are intrinsically very weakly clustered, more than $10\times$ less clustered than the LBGs at $\mathcal{R} \sim 25.5$ (e.g. Brainerd, Smail, & Mould 1995),

they provide a reasonable approximation to a random distribution, and they have the advantage of being subject to similar angular variations in detection probability as our LBG sample. As can be seen in Table 2, the difference between measures of $w(\theta)$ (from the same estimator) obtained using the random distribution or the cross-correlation technique described above is comparable to the random error and does not show any systematic trend, suggesting that the effect discussed here is not important at the current level of precision of the data.

Variations of sensitivity or in the photometric calibration (particularly in the U_n band) across individual fields are another possible source of spurious clustering signal. This is because the density of objects with $U_n - G$ and $G - \mathcal{R}$ colors close to edge of the color selection “window” is relatively high, and small variations in the photometry can result in a significant number of galaxies being excluded from or included in the sample. Small spatial variations in sensitivity or color are most likely to have the same dependence as the \mathcal{R} detection probability, as they would be due to small amounts of vignetting and/or variation in image quality that would affect all bandpasses in a similar fashion, to first order. The quality of the CCDs used to obtain the images is high enough that spatial variation in quantum efficiency, even in the U_n band, are small enough so as to be negligible in this context. Moreover, our photometric selection criteria are conservative enough that any objects scattering into or out of our selection window would also be bona fide LBGs, and their redshift distribution would not be different enough to have a significant effect on the clustering properties. That is, small spatial variations in the color zero point could have only a second-order effect on the clustering properties, given that the transformation of the angular into the spatial correlation function depends relatively weakly on the redshift distribution.

3.3. Field Geometry

Two of our fields, SSA22 and DSF2237, were each constructed from two abutting CCD frames aligned along one direction in order to produce composite samples covering larger area than that of the individual pointings. In general, whether it is advantageous to estimate $w(\theta)$ from one large field with N galaxies or from M subfields with N/M galaxies and then average the results depends on the noise characteristics of the adopted estimator (see Landy & Szalay 1993 for a discussion). If the noise scales as $1/N$, like in the case of the PB estimator, then it would make no difference. Analyzing the abutting fields separately instead of together increases the total noise by a factor of M in the case of the LS estimator, because its variance scales as $1/N^2$. Furthermore, in both cases an additional error is also introduced by the $1/M$ loss in the total pairs. Thus, the combination of composite fields and the LS statistics offers the possibility of extracting $w(\theta)$ from the data maximizing the S/N, which is useful in cases like ours where the samples are still relatively small and the clustering signal rather weak.

Unfortunately, fluctuations of the apparent galaxy surface density from field to field due to images of differing depths, galactic extinction and reddening, and so on, can introduce an artificial clustering signal in the observed $w(\theta)$ and cancel the benefits of using composite fields. Although

a relatively large overlapping region between the two individual images that compose these fields allowed us to check the consistency of the photometry and selection criteria between them, the possibility that the two sub-fields have slightly different depth is difficult to test. Therefore, we have studied both cases of split and composite fields with both the PB and LS statistics, each time using both the random and cross-correlation techniques. The results are listed in Table 2. It can be seen that, in every case, $w(\theta)$ in the case of composite fields is shallower and with a larger correlation amplitude than that from the split fields, whose parameters also have larger random errors. Although the difference is comparable to the $1\text{-}\sigma$ error bars, making the results still consistent with each other, there is a possible presence of a systematic error from this effect.

3.4. The PB estimator vs the LS estimator

Table 2 and Figure 2 show that the measures of $w(\theta)$ obtained using the PB estimator are systematically larger than those from the LS one, with the fractional difference between the two statistics being the largest at separations of the order of ~ 100 arcsec. As a result, the correlation function obtained using the PB statistics has a shallower slope and larger correlation amplitude, and the random errors on the fitted parameters are smaller. Again, such differences are comparable to the $1\text{-}\sigma$ error bars and, formally, the parameters derived from the two estimators agree with each other. However, it is clear that the difference is systematic. It is beyond the scope of this paper to analyze the relative merits of the two estimators, and here we simply report all the results, cautioning that the discrepancy that we found, although comparable to the random errors, may imply that the two statistics are sensitive to the presence of low-level systematics in different way.

4. THE INVERSION OF THE ANGULAR FUNCTION

The angular correlation function $w(\theta)$ can be obtained from the spatial one, $\xi(r)$, through the Limber transform if the galaxies' redshift distribution dN/dz is known (Peebles 1980; Efsthathiou *et al.* 1991). If the spatial function can be modeled as

$$\xi(r) = (r/r_0)^{-\gamma} \times f(z), \quad (5)$$

where $f(z)$ describes its redshift dependence, the angular function has the form $w(\theta) = A_w \theta^{-\beta}$, where $\beta = \gamma - 1$ and

$$A_w = C r_0^\gamma \int_{z_i}^{z_f} f(z) D_\theta^{1-\gamma}(z) \left(\frac{dN}{dz} \right)^2 g^{-1}(z) dz \times \left[\int_{z_i}^{z_f} \left(\frac{dN}{dz} \right) dx \right]^{-2} \quad (6)$$

(Efsthathiou *et al.* 1991). Here $D_\theta(z)$ is the angular diameter distance,

$$g(z) = \frac{c}{H_0} [(1+z)^2 (1 + \Omega_0 z)^{1/2}]^{-1}, \quad (7)$$

and C is a numerical factor given by

$$C = \sqrt{\pi} \frac{\Gamma[(\gamma - 1)/2]}{\Gamma(\gamma/2)}. \quad (8)$$

The Lyman-break galaxies’ redshift distribution is considerably narrower than those of traditional flux-limited redshift surveys and spans a redshift interval of only $\Delta z \sim 0.8$ (the corresponding cosmic-time interval is $\approx 0.35 h^{-1}$ ($0.26 h^{-1}$) Gyr for $q_0 = 0.1$ ($q_0 = 0.5$)). In this redshift range and at the spatial scales considered here (larger than a few Mpc), the evolution of cosmic structure is largely driven by the growing mode of linear perturbations $D(t)$. The front-to-end fractional variation of $D(t)$ in the above redshift range is ~ 13 (18%), which is an upper limit to the effective variation of the correlation length in our sample because of the peaked redshift distribution. It is reasonable, therefore, to expect little evolution of LBG clustering in our sample over so short a time. In this case the function $f(z)$ above can be taken out of the integral and the quantity $r_0(z) = r_0 f(z)$ is then the correlation length at the epoch of observations.

We list in Table 3 the comoving correlation lengths $r_0(z)$ at $\bar{z} = 3.04$ obtained through Eqn. (6) using the average $w(\theta)$ and the redshift distribution $N(z)$ plotted in Figure 1. The 68% confidence intervals were computed using Monte Carlo simulations. As mentioned above, the correlation length turns out to be much more tightly constrained than the individual parameters of the angular correlation function, with a typical fractional error of ≈ 20 –30% at the $1\text{-}\sigma$ level. This is enough precision to show the effects of the systematic differences between the values of r_0 obtained from the PB and LS statistics and between keeping the two adjacent pointings in the SSA22 and DSF2237 fields as independent or joining them into two composite fields, respectively. Figures 3a and 3b shows the distribution of values of r_0 obtained combining together the measures of r_0 from the Monte Carlo simulations for the PB (thin continuous histogram) and LS estimators (broken histogram) respectively, for the two values of q_0 considered in the paper. We defer a deeper analysis of the systematics to future papers. At this time, because the differences between all the various measures of r_0 that we have obtained are still comparable to the $1\text{-}\sigma$ random errors, we list them all. As our fiducial measure and error bar we adopt the median of the distribution obtained by merging the PB and LS Monte Carlo distributions and its corresponding 68% confidence interval. These are $r_0 = 3.3_{-0.6}^{+0.7}$ and $r_0 = 2.1_{-0.5}^{+0.4} h^{-1}$ Mpc for $q_0 = 0.1$ and $q_0 = 0.5$, respectively, and the histograms of these distributions are plotted in Figure 3 as thick continuous lines. We have used these values to produce the plots in Figure 4. Our fiducial value of β , obtained in a similar fashion is $\beta = 0.98_{-0.28}^{+0.32}$ and the histograms of the Monte Carlo simulations for the PB, LS and combined samples are plotted in Figure 3c. Finally, we remind that all values of correlation length would be approximately 25% higher in the case of “maximum contamination.”

We can estimate the bias of these galaxies by comparing their correlation function ξ_g to the correlation function of the mass ξ_m :

$$b(r) = \sqrt{\frac{\xi_g(r)}{\xi_m(r)}}. \quad (9)$$

Although (as eq. 9 shows) the bias is in principle a function of scale, our constraint on the power-law exponent $\gamma \equiv 1 - \beta$ is relatively weak (see Table 3), and we can only estimate a “typical” value of the bias over the scales of a few Mpc which are probed here. In practice, we use the ratio of the correlation length of the LBGs to that of $\xi_m(r)$ predicted by the CDM theory to compute the bias, which is therefore relative to $r = 1 h^{-1}\text{Mpc}$. Using a CDM power-spectrum with shape parameter $\Gamma^* = 0.25$, claimed to fit the shape of the local large-scale structure very well (Peacock 1997), and normalization of Eke, Cole, & Frenk (1996), we estimate $b \sim 1.5$ (4.5) for $q_0 = 0.1$ (0.5). Choosing $\Gamma^* = 0.20$ results in $b \sim 1.5$ (5), while adopting the normalization of White, Efstathiou & Frenk (1993) results in $b \sim 1$ (4).

Overall, these bias values are slightly lower than those estimated in Paper 1, but are consistent with them at the $\sim 10\%$ confidence level.

5. DISCUSSION

The high efficiency of the Lyman-break technique and the relatively narrow range of redshifts/cosmic time that it probes make angular clustering a particularly economic means to study large-scale structure at high redshifts, once the redshift distribution of the galaxy candidates has been measured. Not only is one free from securing a complete spectroscopic follow-up of the candidates, but the systematics due to selection effects are easier to handle than those that affect studies of spatial clustering using the full redshift information. Our two main conclusions from an analysis of the angular clustering of Lyman-break galaxies in the redshift range $2.5 \lesssim z \lesssim 3.4$ are that these systems are strongly clustered and that their correlation function has a slope which is as steep or steeper than that of local galaxies.

In this section, we discuss the implications of these conclusions in turn.

5.1. The Slope of The Correlation Function

The correlation function of the Lyman-break galaxies has a slope that is comparable to or steeper than that measured at intermediate and low redshifts. Table 2 shows the values of β obtained from the various techniques discussed above for each of the PB and LS estimators, respectively. Combining all the PB Monte Carlo distributions together, we found $\beta_{PB} = 0.80^{+0.25}_{-0.19}$, where the error bars are the 68% confidence interval. Within the errors, this is the same value found for field galaxies in flux selected surveys. The LS estimator returns a slightly steeper correlation function, with $\beta_{LS} = 1.14^{+0.29}_{-0.23}$, comparable to that of the earliest (E/S0) and/or most luminous local galaxies (e.g. Loveday *et al.* 1995). Combining all the Monte Carlo distributions together we found $\beta = 0.98^{+0.32}_{-0.28}$. The distribution of the PB slope rules out $\beta = 0.25$ or shallower at the 99.9% confidence level, while the distribution of the LS slopes rules out $\beta = 0.49$ or shallower at the same confidence level.

The evolution of the slope of the correlation function of the mass (or, equivalently, that of the power spectrum at small scales) has a pronounced dependence on Ω . For a CDM-like power spectrum, it depends very weakly on the shape parameter Γ^* and, for flat models, on the normalization. As Eqn.(9) shows, the slope of $\xi_g(r)$ differs from that of $\xi_m(r)$ because of the dependence of the bias parameter $b(r)$ with the spatial scale. The form of $b(r)$, its dependence on galaxy properties and how it evolves with redshift are still subjects of discussion (e.g. Mann, Peacock & Heavens 1997; Bagla 1997). If the scale dependence of $b(r)$ for the LBGs over the spatial scales probed by our correlation analysis, namely $1 \lesssim r \lesssim 10 h^{-1}\text{Mpc}$, is similar to that of the local galaxies, then our measures of $\gamma = \beta + 1$ are inconsistent with $\xi_m(r)$ from the CDM theory if $\Omega = 1$. With our choice of $\Gamma^* = 0.25$ we found $\gamma_m = 1.25$ (over the range $1 < r < 10 h^{-1}\text{Mpc}$), independently of the normalization. As mentioned above, the dependence on Γ^* is very weak. If $\Gamma^* = 0.1$ then $\gamma_m = 0.98$, while if $\Gamma^* = 0.6$, then $\gamma_m = 1.14$. Using the slope measured from the PB estimator, the steepest CDM slope ($\gamma_m = 1.25$) is ruled out by our data at the 99.90% confidence level. Using the measures from the LS estimator, it is ruled out at the 99.991% confidence level. Open CDM models with the same parameters as above produce slopes in the range $1.6 < \gamma_m < 2.1$ (in open models the slope of $\xi_m(r)$ has a more pronounced dependence on the normalization), which are all consistent with our data.

The above computations assume a bias constant with spatial scale. We stress, however, that the evolution of the slope of the correlation function is useful for constraining cosmological models only if the dependence of the bias with the spatial scale and its evolution with redshift are known. The function $b(r)$ also depends on the properties of the halos, which further complicates the interpretation of the data because of the difficulty of establishing an evolutionary sequence between the systems observed at high redshifts and the local galaxies. Bagla’s (1997) N-body simulations seem to suggest that the bias will not be strongly scale-dependent —his $b(r)$ for $M \geq 2 \times 10^{12} M_\odot$ halos at $z = 0$ in standard CDM has a power-law slope of only ~ -0.18 — and if $b(r)$ for Lyman-break galaxies is similarly flat, our conclusions about the slope would not be importantly changed. But until more is known about the scale-dependence of the bias they will remain speculative.

5.2. Spatial Clustering and its “Evolution”

The LBGs at $z \sim 3$ are characterized by strong spatial clustering, with a co-moving correlation length of $\sim 3 - 4h^{-1} \text{Mpc}$ for a low matter density ($\Omega_0 = 0.2$) Universe. The correlation length would be $\sim 25\%$ higher if the “maximum contamination” applies. This is comparable to the clustering of present-day spiral and IRAS galaxies, and a factor of ≈ 2 smaller than that of present-day ellipticals.

A simple comparison of the observed clustering properties with the expected clustering of a suitably normalized CDM density field, as shown in Figure 3b, suggests that, in the context of such models, the LBGs must be substantially biased with respect to the dark matter, with higher bias

required in models with higher matter density. This result is in qualitative agreement with our conclusions in Paper 1 on the basis of the clustering in redshift space in one of our survey fields, although the redshift-space analysis may imply somewhat higher bias (on slightly different scales) than the correlation function analysis presented here. As discussed there, the strong clustering and the large bias of the Lyman-break galaxies are consistent with biased galaxy formation theories and provide additional evidence that these systems are associated with massive dark matter halos.

One might be tempted to try to fit the Lyman break galaxy clustering properties onto an general evolutionary sequence for galaxy clustering versus cosmic epoch. Figure 4a shows the galaxy clustering strength measured from various redshift surveys, including the LBGs, as a function of redshift. To quantify the clustering strength we have used the function $r_0^{\gamma} \times (1+z)^3$, where now r_0 is in *proper* coordinates. Figure 4b shows the corresponding plot of the bias derived using the CDM mass correlation function, which we have computed using the non-linear code for the evolution of the power spectrum by Peacock (1997). We used the shape parameter $\Gamma^* = 0.25$ and normalized the power spectrum to $\sigma_8 = 1.0$ for the open model and $\sigma_8 = 0.5$ in the Einstein-de Sitter case. The error bars have been computed by propagating the errors in the measure of the correlation length, but it is clear that the dominant uncertainty is in the choice of normalization of the theoretical curve.

As Figure 4 suggests, the variations in the value of the “effective” bias from sample to sample complicate the interpretation of the apparent evolution of galaxy clustering as due to the gravitational growth of structures, preventing us from deriving information on the clustering evolution of the mass. For example, the data show that the traditional power-law model $\xi(r, z) = \xi_0(r) \times (1+z)^{-(3+\epsilon)}$ used to describe the gravitational evolution of clustering (Peebles 1980) is not a good representation for any value of ϵ over the redshift interval $0 \lesssim z \lesssim 3$. In fact, it is clear from N-body simulations (e.g., Brainerd & Villumsen 1993, Bagla 1997) that the behavior of the clustering of *halos*, as opposed to that of the overall mass, will have a non-trivial dependence on redshift that is not accounted for in the “ ϵ ” models. When one also notes the uncertainties in the way in which dark halos are effectively sampled in any given redshift survey, we question the ultimate usefulness of fitting values of this parameter to the results of redshift surveys over substantial redshift baselines.

Lyman-break galaxies at $z \sim 3$ represent both a large jump in redshift and a substantially different detection/selection technique than has been used previously in most of galaxy clustering analyses. It is highly likely that a similar selection criterion applied to nearby galaxies would result in a very different correlation function than for (nearby) optically-selected galaxies. If star formation progresses to less massive systems with time (e.g., Cowie *et al.* 1997, Giavalisco *et al.* 1996), then a Lyman-break galaxy sample over a large range of redshifts would likely exhibit a gradually *diminishing* clustering strength with time, rather than a monotonically increasing clustering strength due to growth of the overall mass fluctuations due to gravitational instability. Our results emphasize that the interpretation of apparent “evolution” of the clustering properties of galaxies in deep surveys (e.g., Efstathiou 1995; Brainerd *et al.* 1995, etc.) cannot be directly

interpreted as a reliable measure of the overall growth of structure. In a typical survey limited by apparent magnitude, the mix of galaxy types and the relative sensitivity of the survey to stellar mass, star formation rate, and bolometric luminosity (and the complicated manner in which these quantities are related to overall galaxy mass) will be strongly redshift-dependent. It is apparent now, if it has not always been, that the clustering properties of galaxies at moderate to high redshift cannot be used as a cosmological tool unless one is prepared to simultaneously understand where galaxies form and how they evolve relative to the underlying distribution of dark matter—cosmology and galaxy formation cannot be understood independently in this context.

These problems argue strongly in favor of a focused approach to studies of large-scale structure over substantial redshift baselines, and call into question the very use of the phrase “evolution of galaxy clustering”. The results found in this paper reiterate that selecting a particular class of objects as defined by their observational properties, over a relatively narrow range of cosmic time, may offer the best hope of constructing meaningful samples for clustering analyses that can be compared with theoretical predictions (e.g. Le Fevre *et al.* 1996; Carlberg *et al.* 1997). At very high redshifts the specific mechanisms of galaxy formation are expected to affect the clustering of forming systems the most. In the case of the $z \sim 3$ LBGs, the interval of cosmic time spanned by such samples are small enough, and the selection criterion uniform enough, that even if it may be quite model-dependent to “map” them onto samples of galaxies selected differently at other redshifts, one might at least be confident of measuring something specific that can be easily compared to the predictions of models or simulations (e.g. Adelberger *et al.* 1998, Giavalisco *et al.* 1998b, in prep.).

Because the LBG selection technique (or other equivalent to it) is sensitive to those galaxies that are the most actively star-forming systems (at whatever redshift/epoch probed), understanding the evolution of the clustering with redshift would involve not only the modeling of the underlying dark matter distribution, which is now relatively straight-forward using N-body simulations, but also a detailed understanding of which types of objects (i.e., which “halos”) would be harboring star formation at detectable levels as a function of time. Simulations that include star formation (e.g., Baugh *et al.* 1997, Weinberg *et al.* 1997) can make direct predictions of the clustering properties of objects subject to a star formation rate threshold, based on semi-analytic treatment of star formation within dark matter halos. The observed clustering strength of LBGs is close to predictions of these models (particularly after possible corrections for a small amount of contamination in the photometrically selected LBG sample), and similar numbers result naturally from pure N-body or analytic models that assume a mapping of the most massive virialized halos at $z \sim 3$ to objects likely to be visible because of their star formation (Bagla 1997, Mo & Fukugita 1996, Jing & Suto 1997).

Our current measurements can be improved upon in a number of ways. First, obtaining photometric identifications of LBGs over much larger fields would result in much better independent constraints on the amplitude and slope of the angular correlation function. Secondly, a full real-space analysis of the clustering properties of the LBGs in the same fields will offer a

much higher signal-to-noise ratio (and a different dependency on cosmological parameters) than can be attained from the angular distribution of candidates coupled with an empirical redshift selection function. The real-space analysis requires a more careful treatment of observational selection effects, and reasonably complete spectroscopy, and we have deferred this to a future paper (Adelberger *et al.* 1998).

6. SUMMARY

We have measured the angular correlation function $w(\theta)$ of Lyman-break galaxies at redshift $z \sim 3$. Fitting the power-law $A_w \theta^{-\beta}$ to a weighted average of $w(\theta)$ from the five fields over the range $12 \lesssim \theta \lesssim 330$ arcsec, we find $A_w \sim 2$ arcsec $^\beta$ and $\beta \sim 0.9$. The slope is, within the errors, the same as for galaxy samples in the local and intermediate redshift universe, and a slope $\beta = 0.25$ or shallower is ruled out by the data at the 99.9% confidence level.

Because the redshift distribution $N(z)$ of LBGs is well determined from 376 spectroscopic redshifts, we have derived the real-space correlation function from the angular one through the Limber transform. The inversion of the $w(\theta)$ is rather insensitive to the still relatively large uncertainties on A_w and β , and the spatial correlation length r_0 is much more tightly constrained than these. Using Monte Carlo simulations to derive the 1σ error bars from the 68% confidence interval, we estimate $r_0 = 3.3_{-0.6}^{+0.7}$ ($2.1_{-0.5}^{+0.4}$) h^{-1} Mpc (comoving) for $q_0 = 0.1$ (0.5) at the median redshift of the survey, $\bar{z} = 3.04$. Thus, the observed comoving correlation length of LBGs at $z \sim 3$ is comparable to that of present-day spiral galaxies and is only $\sim 50\%$ smaller than that of present-day ellipticals; it is as large or larger than any measured in recent intermediate-redshift galaxy samples ($0.3 \lesssim z \lesssim 1$).

By comparing the observed correlation length of LBGs to that of the mass predicted from CDM theory, we have estimated a linear bias for LBGs of $b \sim 1.5$ (4.5) for $q_0 = 0.1$ (0.5), in broad agreement with our previous estimates based on preliminary spectroscopy (Paper 1). The strong clustering and the large inferred bias of the LBGs are consistent with biased galaxy formation theories and provide additional evidence that these systems are associated with massive dark matter halos.

The evolution of the slope of the correlation function of the mass (or, equivalently, that of the power spectrum at small scales) has a pronounced dependence on Ω . If the biasing parameter is a weak function of the spatial scale, the measured slope of the correlation function of LBGs, $\gamma = 1.98_{-0.28}^{+0.32}$, is inconsistent with the predictions of the standard CDM theory with $\Omega = 1$ at the 99.9% confidence level. N-body simulations seem to suggest that the bias will not be strongly scale-dependent; however, until more is known about the scale-dependence of the bias, this conclusion will remain speculative.

The results of the clustering of LBGs at $z \sim 3$ emphasize that apparent evolution in the clustering properties of galaxies may be due as much to variations in effective light-to-mass

bias parameter among different galaxy samples as to evolution in the mass distribution through gravitational instability. Our study shows that the traditional power-law model $\xi(r, z) = \xi_0(r) \times (1+z)^{-(3+\epsilon)}$ traditionally used to describe the gravitational evolution of clustering (Peebles 1980) is not a good representation for any value of ϵ over the redshift interval $0 \lesssim z \lesssim 3$.

We are grateful to an anonymous referee for useful comments and suggestion that have improved our paper. We would like to thank the staff at the Palomar, Kitt Peak and Keck observatories for their invaluable help in obtaining the data that made this work possible. We are greatly indebted to Ed Carder at KPNO for understanding the cause of the $CuSO_4$ leakage in the U_n filter and his superb work in repairing it. We have benefited from stimulating conversations with Ray Carlberg, John Peacock and Cedric Lacey, who have also kindly made available to us their theoretical models of CDM clustering evolution. We are grateful to Richard Ellis for his useful comments on an early version of the paper. MG has been supported by the Hubble Fellowship program through grant HF-01071.01-94A awarded by the Space Telescope Science Institution, which is operated by the Association of Universities for Research in Astronomy, Inc. under NASA contract NAS 5-26555. CCS acknowledges support from the U.S. National Science Foundation through grant AST 94-57446, and from the Alfred P. Sloan Foundation.

REFERENCES

- Adelberger, K. L., Steidel, C. C., Giavalisco, M., Dickinson, M. E., Pettini, M., & Kellogg, M. 1998, ApJ, submitted.
- Bagla, J. S. 1997, MNRAS, submitted, astro-ph/9711081
- Baugh, C. M., Cole, S., Frenk, C. S., & Lacey, C. G. 1998, ApJ, in press, astro-ph/9703111
- Brainerd, T. G. & Villumsen, J. V. 1994, ApJ, 431, 477
- Brainerd, T. G., Smail, I., & Mould, J. 1995, MNRAS, 275, 781
- Carlberg, R. G., Cowie, L. L., Songaila, A., Hu, E. M. 1997, ApJ, 484, 538
- Cohen, J. G., Cowie, L. L., Hogg, D. W., Songaila, A., Blandford, R., Hu, E. M., Shopbell, P. 1996, ApJ, 471, L5
- Connolly, A. J., Csabai, I., Szalay, A. S., Koo, D. C., Kron, R. G., & Munn, J. A. 1995, AJ, 110, 2655
- Connolly, A. J., Szalay, A. S., Dickinson, M. E., Subbarao, M., U., & Brunner, R. J. 1997, ApJ, 486, L11
- Cowie, L. L., Hu, E. M., & Songaila, A. 1995a, Nature, 377, 603
- Cowie, L. L., Songaila, A., Hu, E. M. & Cohen, J. G. 1996, AJ, 112, 839

- Cowie, L. L., Hu, E. M., Songaila, A., & Egami E. 1997, ApJ, 481, L9
- Davis, M., & Peebles, P. J. E. 1983, ApJ, 267, 465
- Davis, M., Efstathiou, G., Frenk, C., & White, S. D. M. 1985, ApJ, 292, 371
- Davis, M., Meiksin, A., Strauss, M. A., Da Costa, N. L., & Yahil, A. 1988, ApJ, 333, L9
- Efstathiou, G., Bernstein, G., Katz, N., Tyson, A. J., & Guhathakurta, P. 1991, ApJ, 380, L47
- Efstathiou, G., 1995, MNRAS, 272, L25
- Eke, V. R., Cole, S., & Frenk, C. S. 1996, MNRAS, 282, 263
- Giavalisco, M., Steidel, C. C., & Macchetto 1996, ApJ, 470, 189
- Groth, E. J., & Peebles, P. J. E. 1977, ApJ, 217, 385
- Governato, F., Baugh, C. M., Frenk, C. S., Lacey, C. G., Quinn, T., & Stadel, J. 1998, preprint
- Hamilton, A. J. 1988, ApJ, 331, L59
- Jing, Y. P., & Suto, Y. 1998, ApJ, submitted, astro-ph/9710090
- Landy, S.D. & Szalay, A.S., 1993, ApJ, 412, L64
- Landy, S.D. & Szalay, A.S., & Koo, D. C. 1996, ApJ, 460, 94
- Le Fèvre, O., Hudon, D., Lilly, S. J., Crampton, D., Hammer, F., & Tresse, L. 1996, ApJ, 461, 534
- Lilly, S., Tresse, L., Hammer, F., Crampton, D., & Le Fèvre, O. 1995, ApJ, 455, 108
- Ling, E. N., Barrow, J. D., Frenk, C. S. 1986, MNRAS, 223, L21
- Loveday, J., Maddox, S. J., Efstathiou, G., & Peterson, B. A. 1995, ApJ, 442, 457
- Lowenthal, J. D., Koo, D. C., Guzman, R., Gallego, J., Phillips, A. C., Faber, S. M., Vogt, N. P., Illingworth, G. D., Gronwall, C. 1997, ApJ, 481, 673
- Madau, P., 1995, ApJ, 441, 18
- Madau, P. Ferguson, H. C., Dickinson, M. E., Giavalisco, M., Steidel, C. C., & Fruchter, A. 1996, MNRAS, 283, 1388
- Madau, P., Pozzetti, L., & Dickinson, M. E. 1997, ApJ, in press, astro-ph/9708220
- Mann, R. G., Peacock, J. A., & Heavens, A. F. 1997, MNRAS, in press, astro-ph/9708031
- Matarrese, S., Coles, P., Lucchin, F., & Moscardini, L. 1997, MNRAS, 286, 115
- Mo, H. J., & Fukugita, M. 1996, 467, L9
- Mo, H. J., & White, S. D. M. 1996, MNRAS, 282, 347
- Oke, J. B., & Gunn, J. E. 1983, ApJ, 266, 713
- Oke, J. B., Cohen, J. G., Carr, M., Cromer, J., Dingizian, A., Harris, F. H., Labrecque, S., Lucinio, R., Schaal, W, Epps, H., Miller, J. 1995, PASP, 107, 375
- Park, C., Vogeley, M. S., Geller, M., & Huchra, J. P. 1994, ApJ, 431, 569

- Peacock, J. A. 1997, MNRAS, 284, 885
- Peebles, P. J. E., 1980 “The Large-Scale Structure of the Universe”, Princeton University Press.
- Press, W. H., Flannery, B. P., Teukolsky, S. A., & Vetterling, W. T. 1992, “Numerical Recipes”, Cambridge University Press
- Santiago, B. X., Da Costa, L. N. 1990, ApJ, 362, 386
- Schade, D., Lilly, S. J., Crampton, D., Hammer, F., Le Fèvre, O., & Tresse, L. 1995, ApJ, 451, L1
- Steidel, C.C., & Hamilton, D. 1993, AJ, 105, 2017 (Paper II)
- Steidel, C.C., Pettini, M., & Hamilton, D. 1995 (Paper III), AJ, 110, 2519
- Steidel, C. C., Giavalisco, M., Pettini, M., Dickinson, M., & Adelberger, K. 1996a, ApJ,
- Steidel, C. C., Giavalisco, M., Dickinson, M., & Adelberger, K. L. 1996b, AJ, 112, 352
- Steidel, C. C., Adelberger, K. L., Dickinson, M. E., Giavalisco, M., Pettini, M., & Kellogg, M. 1998, ApJ, in press, astro-ph/9708125, Paper 1
- Tucker, D. L., Oemler, A., Jr., Kirshner, R. P., Lin, H., Schectman, S. A., Landy, S. D., Schechter, P. L., Muller, V., Gottlober, S., Einasto, J. 1997, MNRAS, 285, L5
- Valotto, C. A., & Lambas, D. G. 1997, ApJ, 481, 594
- Weinberg, D., Katz, N., & Hernquist, L. 1997, in “Origins”, eds. M. J. Shull, C. E. Woodward, & H. Thronson, (ASP Conference series), astro-ph/9708213
- White, S. M., Davis, M., Efstathiou, G., & Frenk, C. S. 1987, Nature, 330, 451
- White, S. M., Efstathiou, G., Frenk, C. S. 1993, MNRAS, 262, 1023

Table 1. The Observed Fields

#	Field	Size ^a	N ^b	\mathcal{N}^c	α^d
1	0050+123 (CDF)	8.8×8.9	80	1.02	59.0
2	1234+625 (HDF)	8.6×8.7	104	1.39	50.9
3	1415+527 (Westphal)	15.1×15.1	293	1.29	52.9
4	2215+000 (SSA22)	8.6×17.6	186	1.23	54.1
4a	2215+000 (SSA22a)	8.6×8.9	87	1.14	56.3
4b	2215+000 (SSA22b)	8.6×9.0	99	1.28	53.1
5	2237+114 (DSF2237)	17.4×10.1	208	1.18	55.2
5a	2237+114 (DSF2237a)	9.2×10.1	86	0.93	62.4
5b	2237+114 (DSF2237b)	9.0×10.1	127	1.40	50.8

^aIn units of arcmin².

^bNumber of LBG candidates with $\mathcal{R} \leq 25.5$.

^cSurface density at $\mathcal{R} \leq 25.5$; galaxies per arcmin².

^dMean intergalaxy angular separation at $\mathcal{R} \leq 25.5$; arcsec.

Table 2. The Fitted Parameters

Estimator	A_w ^a	β ^b
PB rand	$1.3^{+1.2}_{-0.7}$	$0.7^{+0.1}_{-0.1}$
PB rand-split	$2.1^{+3.1}_{-1.2}$	$0.9^{+0.2}_{-0.2}$
PB xcor	$1.0^{+1.2}_{-0.6}$	$0.7^{+0.2}_{-0.2}$
PB xcor-split	$2.3^{+4.7}_{-1.5}$	$1.0^{+0.3}_{-0.2}$
PB all	$1.5^{+2.3}_{-0.9}$	$0.8^{+0.3}_{-0.2}$
LS rand	$3.4^{+5.5}_{-2.1}$	$1.1^{+0.3}_{-0.2}$
LS rand-split	$4.1^{+10.0}_{-2.8}$	$1.2^{+0.3}_{-0.3}$
LS xcor	$3.8^{+5.1}_{-2.2}$	$1.1^{+0.2}_{-0.2}$
LS xcor-split	$6.2^{+12.3}_{-4.0}$	$1.3^{+0.3}_{-0.2}$
LS all	$4.1^{+7.8}_{-2.6}$	$1.1^{+0.3}_{-0.2}$
PB + LS all	$2.5^{+5.5}_{-1.7}$	$1.0^{+0.3}_{-0.3}$

^aAngular correlation amplitude in arcsec ^{β}

^bAngular correlation slope

Table 3. The Correlation Length^a

	r_0	r_0
$q_0 = 0.1$	PB	LS
rand	$3.9^{+0.4}_{-0.4}$	$2.9^{+0.4}_{-0.5}$
rand-splt	$3.5^{+0.5}_{-0.5}$	$2.7^{+0.5}_{-0.6}$
xcor	$3.7^{+0.5}_{-0.6}$	$3.3^{+0.5}_{-0.4}$
xcor-splt	$3.1^{+0.5}_{-0.5}$	$2.8^{+0.5}_{-0.5}$
all	$3.6^{+0.5}_{-0.6}$	$2.9^{+0.5}_{-0.6}$
$q_0 = 0.5$		
rand	$2.5^{+0.3}_{-0.3}$	$1.8^{+0.3}_{-0.3}$
rand-splt	$2.3^{+0.2}_{-0.4}$	$1.7^{+0.3}_{-0.3}$
xcor	$2.4^{+0.3}_{-0.4}$	$2.1^{+0.3}_{-0.3}$
xcor-splt	$2.0^{+0.3}_{-0.3}$	$1.8^{+0.3}_{-0.3}$
all	$2.3^{+0.3}_{-0.4}$	$1.9^{+0.3}_{-0.4}$

^aComoving coordinates, in units of h^{-1} Mpc

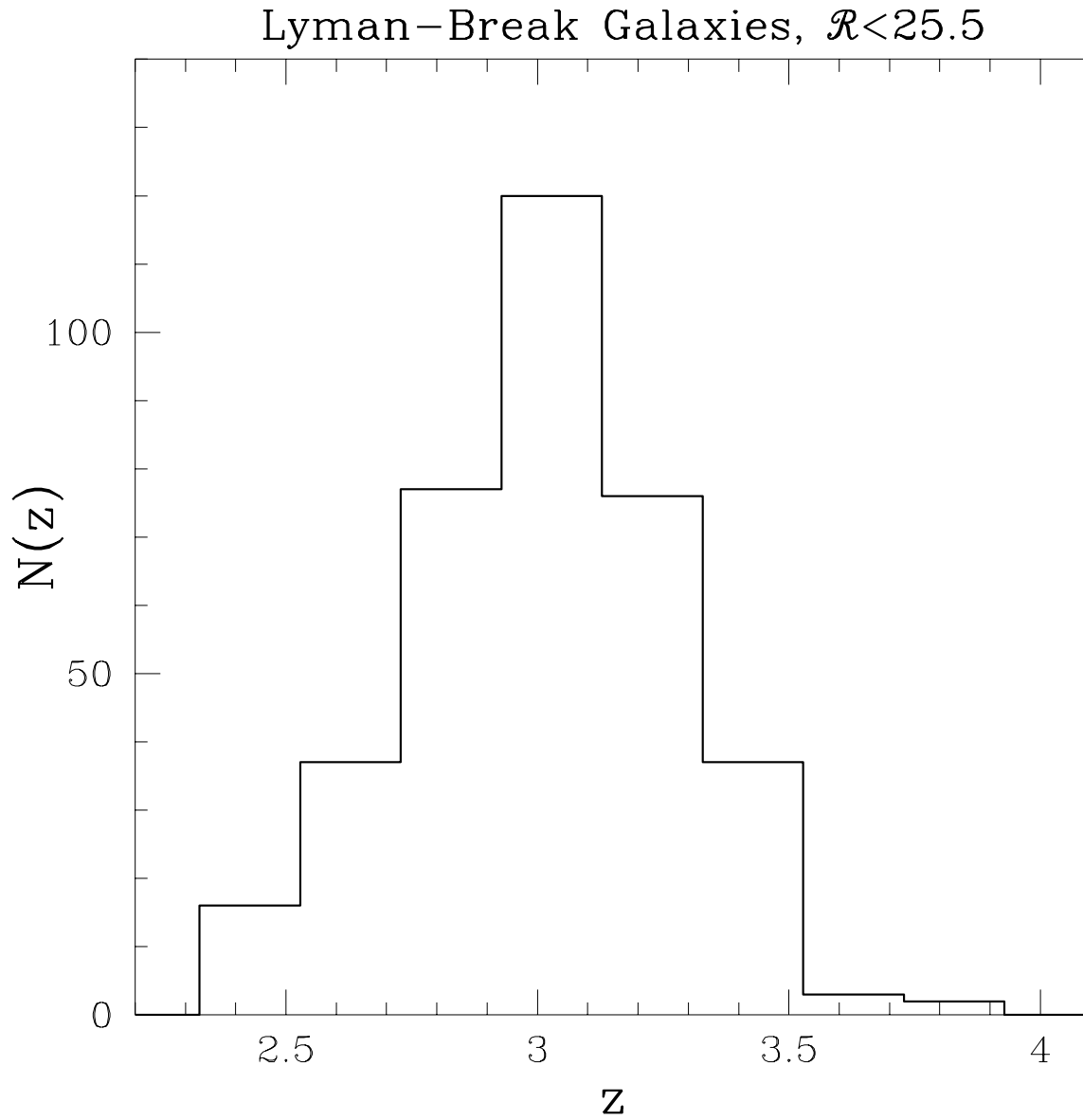


Fig. 1.— The redshift distribution function $N(z)$ of the 376 LBGs used in the correlation analysis. The bin size is $\Delta z = 0.2$. The interval $2.6 \lesssim z \lesssim 3.4$ contains 90% of the galaxies.

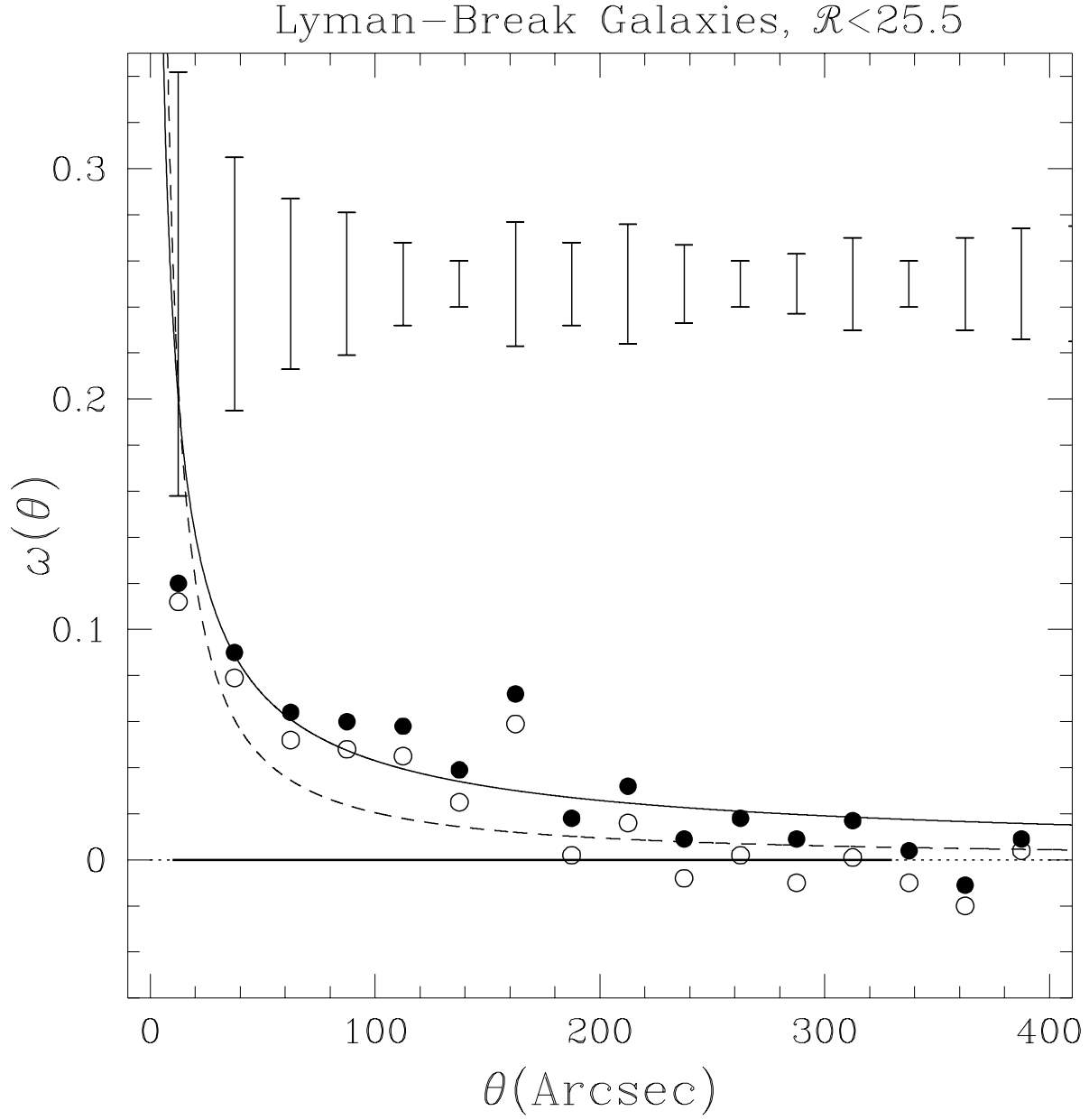


Fig. 2.— Weighted average angular correlation function of LBGs. The filled points are from the PB estimator, the open points from the LS one. The error bars are shown on the top of the figure. The continuous line is the best-fit power law to the PB data points, the dotted line is the fit to the LS. The thick horizontal continuous segment on the x axis marks the angular range over which we computed the fits.

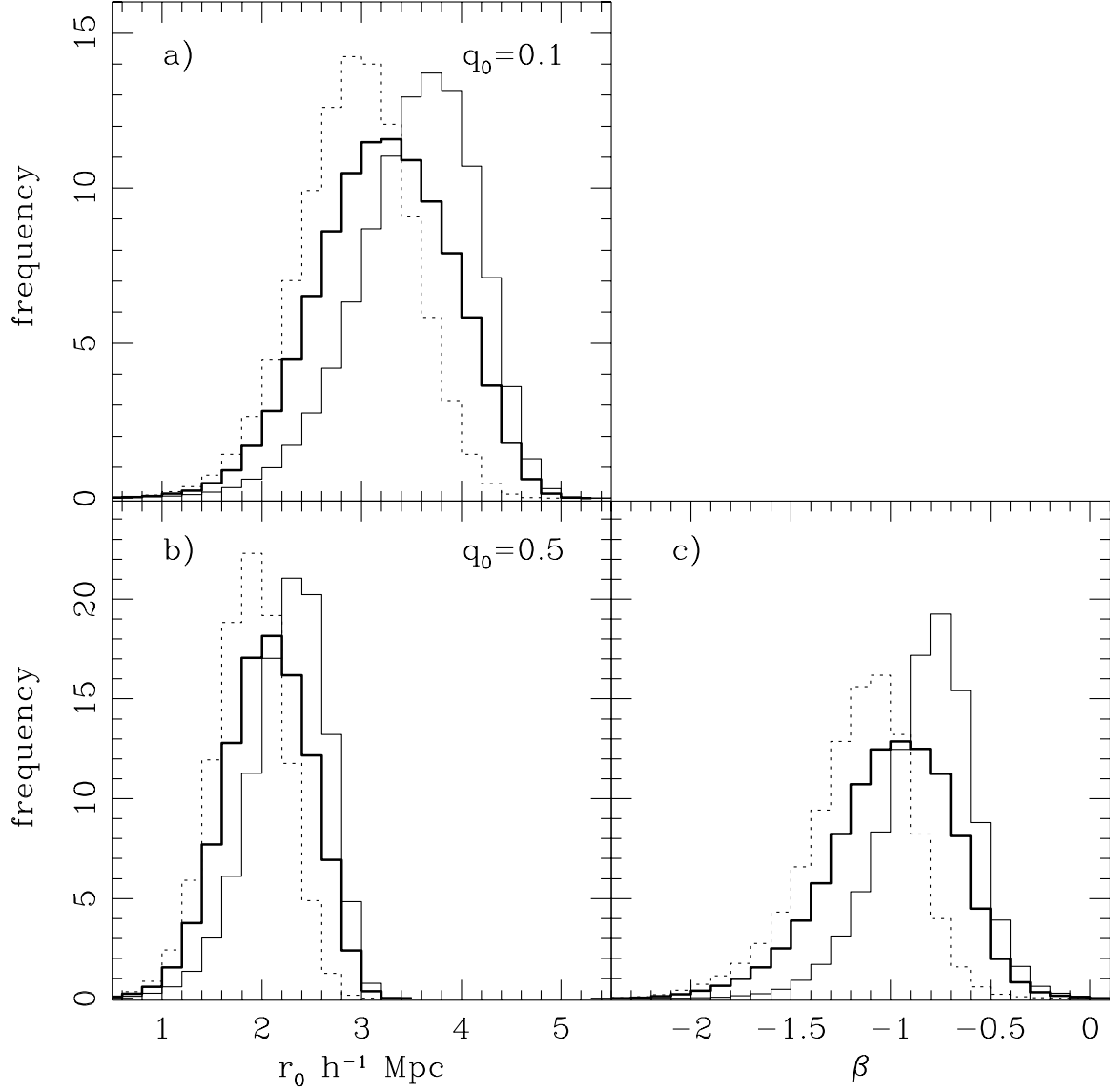


Fig. 3.— The histogram of the correlation length r_0 (a) and b)) and of the slope β (c)) from the Monte Carlo simulations. The thin continuous line is for the PB estimator, the broken line is for the LS estimator. For each estimator, the Monte Carlo distributions corresponding to the four different measures listed in Table 3 have been merged together. The thick continuous line is the distribution of all the PB and LS Monte Carlo samples merged together.

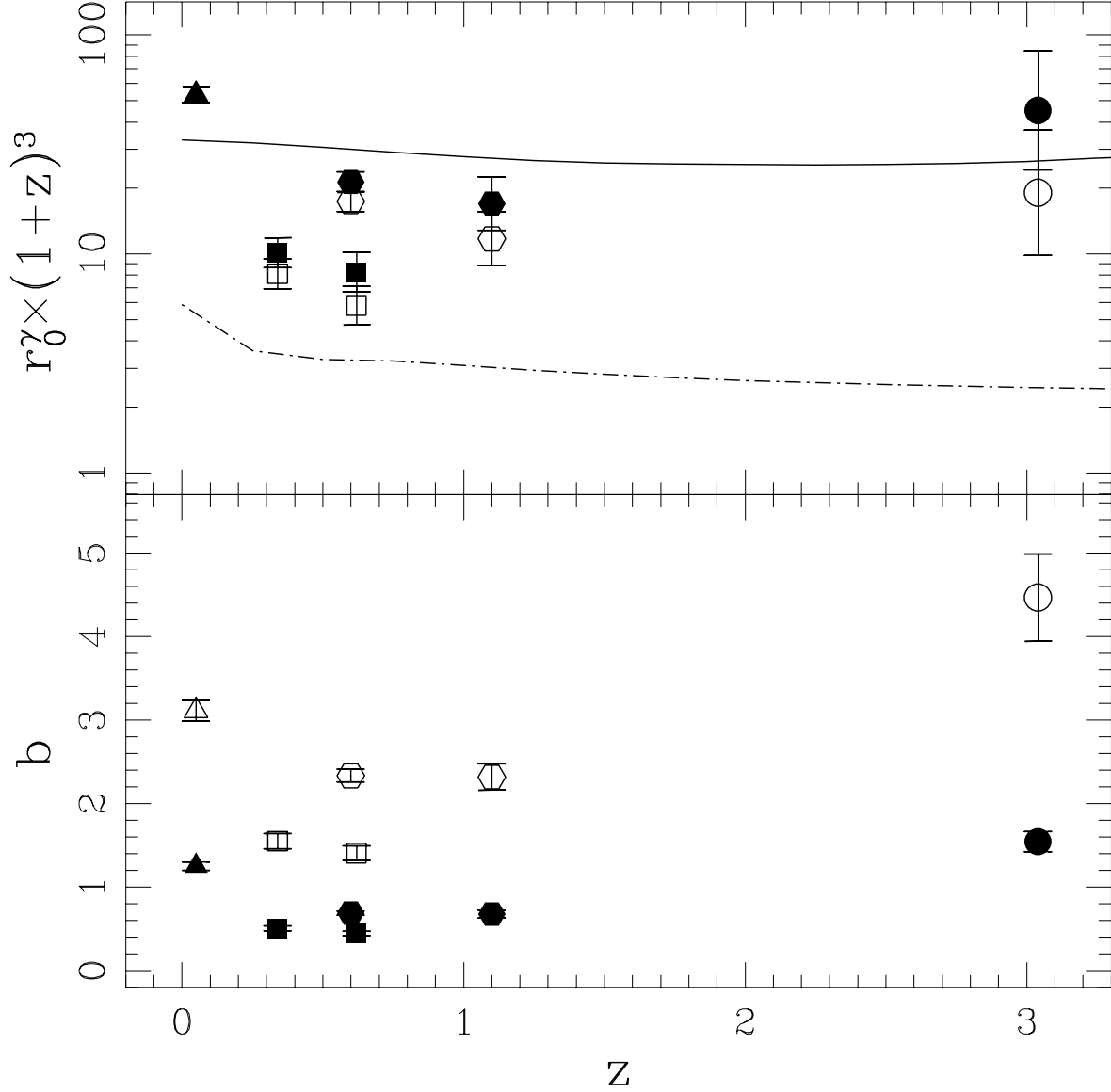


Fig. 4.— **a)** The strength of galaxy clustering as a function of redshift. Filled symbols are for $q_0 = 0.1$, open symbols for $q_0 = 0.5$. Triangles are APM data (Loveday *et al.* 1995), squares are CFRS data (Le Fèvre *et al.* 1996), hexagons Keck K-band data (Carlberg *et al.* 1997), and circles are the LBG data. The continuous solid and dashed lines are the expectations from the CDM theory with $\Gamma^* = 0.25$, $\sigma_8 = 1.0$ and 0.5 for the two case of $q_0 = 0.1$ and 0.5 , respectively. **b)** Linear bias as a function of redshifts for the same data sets as a), assuming the CDM correlation function. Symbols are defined as above.